Optics and Lasers in Engineering 122 (2019) 14–22

Contents lists available at ScienceDirect

Optics and Lasers in Engineering

journal homepage: www.elsevier.com/locate/optlaseng

Small-divergent-angle uniform illumination with enhanced luminance of transmissive phosphor-converted white laser diode by secondary optics design

Yupu Ma, Xiaobing Luo*

School of Energy and Power Engineering, Huazhong University of Science and Technology, Wuhan 430074, China

ARTICLE INFO

Keywords:
Transmissive phosphor
Laser diode
Secondary optics
Uniform illumination

ABSTRACT

With the advantage of low etendue and no efficiency droop, phosphor-converted white laser diode (pc-WLD) has been a very promising candidate in future high-luminance solid-state lighting. To obtain high brightness, the blue laser beam is usually collimated or focused onto a yellow phosphor layer, which may result in poor angular color uniformity (ACU). In this study, we observed the blue spot and yellow ring phenomenon of the transmissive pc-WLD, which is attributed to the mismatch between the focused intensity distribution of the blue light and the divergent intensity distribution of the yellow light. Then, we proposed a secondary optics consisting of a parabolic reflector coupled with a freeform lens to enhance the ACU by collimating all the rays emitting from the phosphor, which is located at the focus of the reflector. Through this design, we achieved the match of the intensity distribution of the blue and yellow lights, resulting in a high ACU of 0.85 with a view angle of ±10° by simulation. Moreover, the luminance of the pc-WLD can be enhanced by about four times using this method. Finally, we fabricated a prototype of the designed secondary optics and validated the effectiveness of the proposed method in achieving small-divergent-angle uniform illumination with enhanced luminance of the transmissive pc-WLD.

1. Introduction

Phosphor-converted white light-emitting diode (pc-WLED) has dominated the solid-state lighting (SSL) industry in the last decade [1–3]. However, LED has been known to suffer from the efficiency droop under high current density [4], which limits the attainable output flux per chip area. As an alternative option of SSL, laser diode (LD) exhibits even higher wall-plug efficiency under high current density [5]. Moreover, LD possesses low etendue due to the directional radiation pattern of laser beam and small light-emitting area [6–8]. The mentioned two points makes the LD a promising candidate in the future high-power and high-luminance SSL [9].

The most common way of achieving white illumination is to use a blue LD to excite a yellow phosphor, which is also called phosphor-converted white laser diode (pc-WLD). There has been two types of pc-WLD, namely the transmissive type [10–15] and the reflective type [16–18]. These two types are defined according to the relative direction of the output white light to the incident blue light [18]. Between them, the transmissive pc-WLD has gained wide adoption with compact size and simple packaging structure. Fig. 1 shows the schematic of a typical transmissive pc-WLD consisting of a blue LD, a collimating lens, and

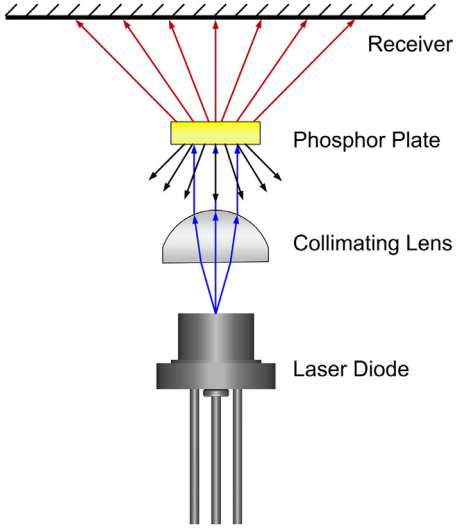

Fig. 1. The schematic of a typical transmissive pc-WLD. The rays marked in blue, red, and black denote the incident laser light, forward scattering light, and backward scattering light, respectively.

* Corresponding author.
E-mail address: luoxb@hust.edu.cn (X. Luo).

https://doi.org/10.1016/j.optlaseng.2019.05.022
Received 11 March 2019; Received in revised form 5 May 2019; Accepted 21 May 2019

a yellow phosphor plate [19]. The blue light emitting from LD is first collimated by the collimating lens to obtain high optical density and thus high luminance. Then, the collimated blue light incidents onto the phosphor plate, which is typically YAG: Ce phosphor. In this process, part of blue light is absorbed by the phosphor particles and then down-converted into yellow light, and the rest of blue light is scattered without being absorbed and transmitted through the phosphor plate. Eventually, the combination of the transmitted yellow light and blue light leads to white light on the receiver [18].

In this configuration, the transmitted blue and yellow lights may exhibit very different spatial intensity distribution, because the blue light is focused with small divergent angle but the yellow light is scattered isotropically in all direction. This raise a question that the angular color uniformity (ACU) of the transmissive pc-WLD may be very poor, resulting in visual discomfort in some typical laser-based lighting applications, e.g., the vehicle headlamp and laser projector. Considering this issue has been rarely studied, it's worthy to give a deep understanding of the angular color performance of pc-WLD. In addition, the forward scattering light is usually used for illumination for the transmissive pc-WLD, but the backward scattering light is wasted, resulting in a reduction in output flux and efficiency.

The secondary optics design may be a potential solution to the mentioned problems by re-distributing the spatial intensity. To enhance ACU, researchers have already proposed some types of freeform lens to achieve uniform illumination of pc-WLED [20,21]. But for transmissive pc-WLD, there has been very few studies. Recently, George et al. have expanded the focused blue laser beam using an expanded lens to excite a large-area phosphor [12]. By using this method, they obtained a high ACU but the luminance is decreased, which is against the unique advantage of the high-luminance illumination using LD. Also, Yang et al. have applied a diffuser to obtain a large-angle uniform illumination but the luminance is sacrificed [13]. An alternative way may be focusing the yellow light to simultaneously enhance ACU and luminance. To reuse the backward scattering lights, a reflector, which is a very common optics in lighting design, can easily reflect them back into the forward direction.

In this work, aimed at improving ACU and luminance of the transmissive pc-WLD, we presented a secondary optics consisting of a parabolic reflector and a freeform lens to focus the yellow light and collect backward scattering light by collimating all the rays emitting from the phosphor. First, the poor angular color performance of the transmissive was investigated using optical simulation. Then, the secondary optics design method was illustrated. Next, the optical performance, including the spatial CCT distribution and luminance, of the pc-WLD integrated with the designed optics was evaluated by simulation, followed by the study of size parameter effect. Finally, we fabricated a prototype of the presented optics and experimentally validated the method by measuring the ACU and luminance.

2. Problem statement

In this section, we evaluate the spatial intensity distribution of the transmissive pc-WLD using the Monto-Carlo ray-tracing simulation. The simulation method is illustrated simply as follows. A commercial LD (L450P1600MM, Thorlabs) is used in this work to excite the phosphor plate. The peak wavelength of LD is 450 nm. The LD is modeled as a grid source with Gaussian spatial intensity distribution with the FWHM divergent angles of 23° and 7° along fast axis and slow axis, respectively. The collimating lens (A110TM-A, Thorlabs) is constructed according to the files provided by the manufacturer. The phosphor plate is a mixture of YAG: Ce phosphor particles and a binder material with corresponding refractive index of 1.80 and 1.53, respectively. The absorption coefficients and scattering coefficients with varying phosphor concentrations are obtained from the Mie theory [22]. The quantum efficiency of the phosphor is assumed to be 0.85. In the simulation, two wavelengths are traced separately, which are 450 nm and 555 nm representing the blue LD light and the down-converted yellow light, respectively. The details of the necessary parameters and simulation process of the YAG: Ce phosphor can be found in our previous work [22,23].

Fig. 2 shows the simulated spatial intensity distribution of the blue and yellow lights emitting from the phosphor in the forward direction. It can be seen that the emitted blue light exhibits a Gaussian distribution with a FWHM divergent angle of 6.4° But the emitted yellow light has a totally different distribution from the emitted blue light. There is a valley in the middle for the yellow light intensity distribution curve and the FWHM divergent angle (116°) is much higher than that of emitted blue light, which is attributed to the isotropic scattering characteristic of the converted yellow light. In addition, the maximum intensity of the emitted yellow is approximately two orders of magnitude smaller than that of the emitted blue light. In this case, the big mismatch between the spatial intensity distributions of the blue and yellow lights will result in very poor spatial color quality, hindering the development of the pc-WLDs in lighting applications where high angular color uniformity is essential. Apart from the poor color mixing effect, there is also another problem need to be addressed. For the transmissive pc-WLD, the output

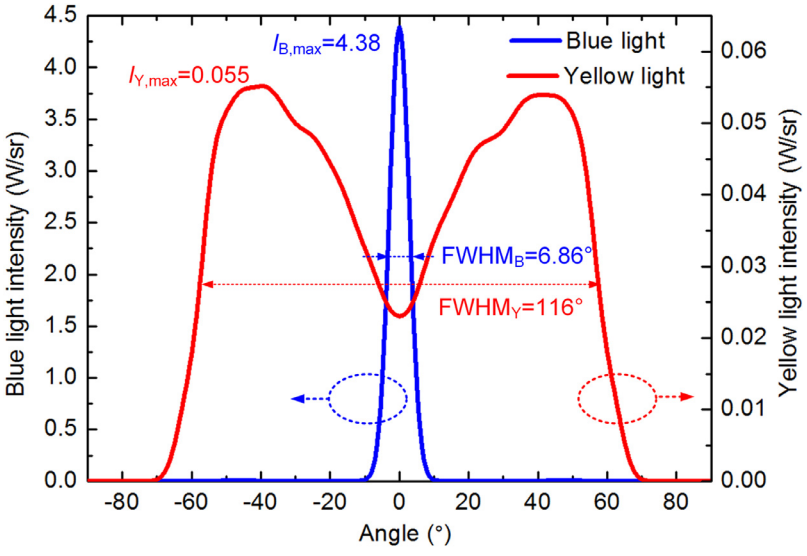

Fig. 2. The simulated spatial intensity distribution of the blue and yellow lights of the transmissive pc-WLD.

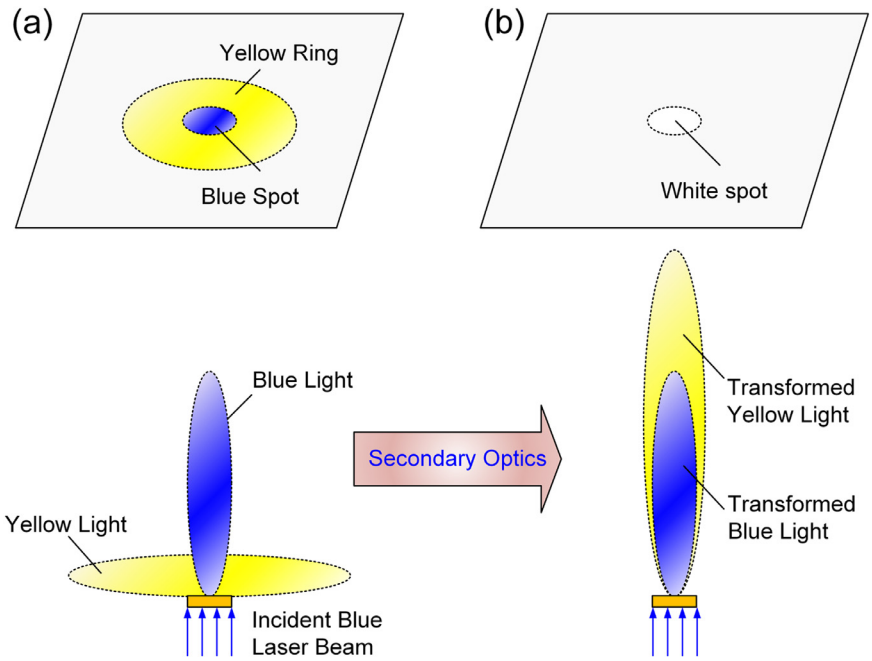

Fig. 3. The transformation of the mismatch between the light distribution of the blue and yellow lights of the transmissive pc-WLD into match of them by secondary optics, leading to enhanced angular color uniformity and luminance for small divergent angle illumination.

light in the forward direction is usually used for illumination and the backward scattering light is wasted, leading to lower optical efficiency and lower luminance.

3. Method definition

3.1. Method principle

To enhance the poor angular color uniformity, the spatial intensity of the blue and yellow lights needs to be re-distributed. Fig. 3 illustrates the transformation of the mismatch between the blue and yellow lights into match of them by secondary optics. As stated above, for the transmissive pc-WLD, the blue light has narrow distribution and the energy is focused in the small-angle region, whereas the yellow light has wide distribution and the energy is distributed in the whole spatial region. As a result, there is a blue spot in the middle and a yellow ring at the edge of the illuminated area on the receiver, which is shown in Fig. 3(a). It's natural to come up with two ways of re-distributing the intensities. One is expanding the blue light distribution and the other is narrowing the yellow light distribution. However, the former method will decrease the luminance. Hence, we choose the later method by simply focusing the yellow light, in which case the blue spot and yellow spot on the receiver are expected to match with each other and generate white spot, as shown in Fig. 4(b). This method is also expected to enhance the luminance by further lowering the etendue of the optical system. To make the best of the scattering light, we can also use the secondary optics to collect the wasted backward scattering light energy, thus enhancing the optical efficiency of the pc-WLD.

To achieve the desired result, we can simply design the secondary optics by beam collimation. As shown in Fig. 4(a), a parabolic reflector (type 1) has been a simple way to collimate light emitting from the focus. However, limited by the finite size of the reflector, the light traveling within small angle will exit directly without collimation. Researchers have combined the reflector with a freeform lens (type 2) to further collimate this part of light [24], as shown in Fig. 4(b). Even so, there is also a waste of the backward scattering light in both cases. Therefore, we further present a modified parabolic reflector coupled with a freeform lens (type 3). In our design, as shown in Fig. 4(c), the phosphor plate is located at the focus of the reflector, and there is a circular hole at the bottom of the reflector allowing the collimated blue laser beam to excite the phosphor. The diameter of the hole is the same as that of the phosphor plate. It should be pointed out that the diffraction effect is not considered when the laser beam passes through the circular hole because the ratio of the laser wavelength to the diameter of the hole is quite small. When the incident blue light hits the phosphor, light will exit from the phosphor in all direction because of scattering. The light can be divided into three parts, namely the forward scattering light in small angle, the forward scattering light in large angle, and the backward scattering light, which are designed to be collimated by the freeform lens, upper parabolic surface, and lower parabolic surface, respectively.

3.2. Constructing the secondary optics

In this section, we introduce the way of constructing the proposed secondary optics, including the modified parabolic reflector and the freeform lens. Both of them possess rotationally symmetric property and can be reduced to a two-dimensional design problem.

Fig. 5 illustrates the parabola of the modified parabolic reflector. We first build a Cartesian coordinate system and the origin is located at the phosphor, which is also the focus of the reflector. It should be noted that the relative size of the phosphor to the reflector has to be small enough to assume the phosphor as a point source. Fortunately, benefiting from the collimated laser beam pattern, the diameter of the phosphor plate can be very small, making the point-source assumption feasible. The parabola can be expressed by the following equation:

$$y = x^2/4f - f \tag{1}$$

where f denotes the focal length. There is another parameter characterizing the parabola, namely the critical angle θ_c, which is defined as the angle between the y-axis and the line from the origin to the vertex of the parabola. Lights traveling along the forward direction with view angle larger than θ_c will be reflected on the parabola and then exit being collimated.

Fig. 6 illustrates the schematic of the 2D structure of the freeform lens. The bottom of the lens is a planar surface and the upper is a freeform surface to be designed. The freeform surface design can be also reduced to design a freeform curve. As shown in Fig. 7, the incident ray $\overrightarrow{OA_1}$ is refracted to $\overrightarrow{A_1B_1}$ by the planar surface, and then $\overrightarrow{A_1B_1}$ is refracted by the freeform curve, and the output ray is collimated.

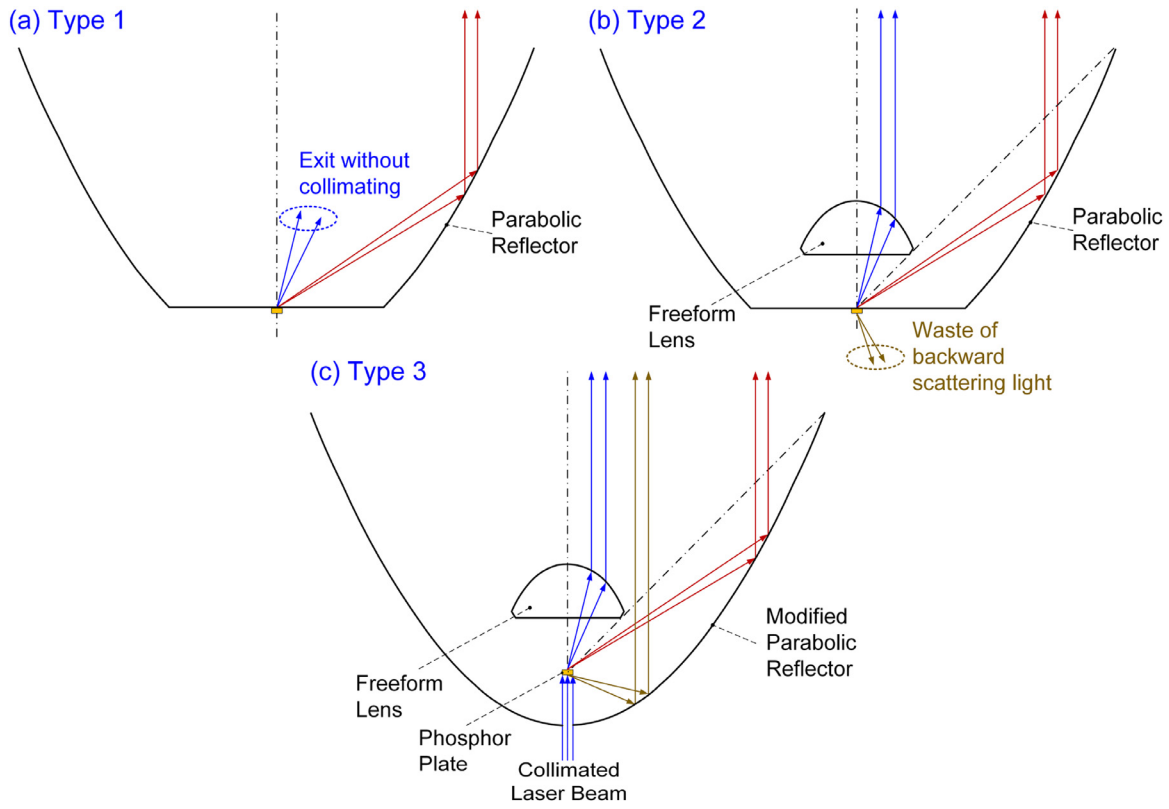

Fig. 4. The schematic and representative light path of three types of secondary optics for beam collimation: (a) type 1 – parabolic reflector, (b) type 2 – parabolic reflector coupled with a freeform lens, and (c) type 3 – the modified parabolic reflector couple with a freeform lens.

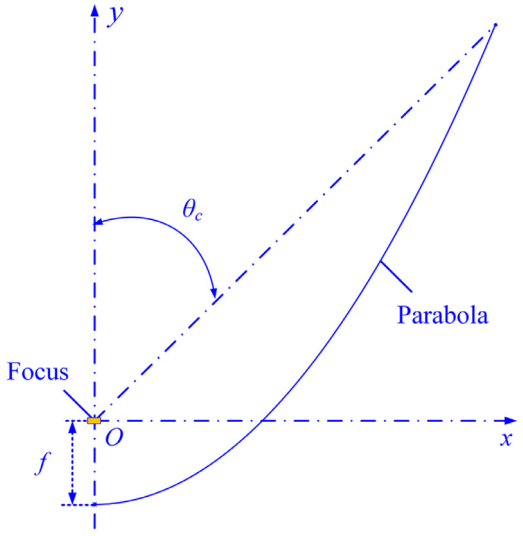

Fig. 5. The schematic of the parabola of the modified parabolic reflector.

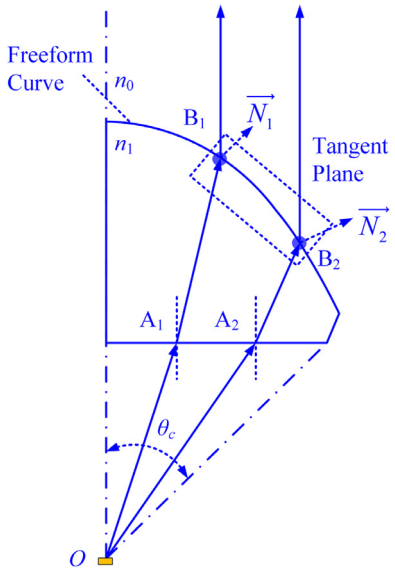

Fig. 6. The schematic of the 2D structure of the freeform lens.

According to the Snell's law, for the freeform curve, the incident ray and the refracted ray satisfies the following equation [25]:

$$\left[1 + n^2 - 2n\left(\overrightarrow{Out} \cdot \overrightarrow{In}\right)\right]^{1/2} \vec{N} = \overrightarrow{Out} - n\overrightarrow{In} \tag{2}$$

where $\overrightarrow{In}$ and $\overrightarrow{Out}$ are the unit vector of the incident ray and output ray, respectively. Because the output ray is designed to be collimated, $\overrightarrow{Out}$ is equal to be {0, 1}. $\vec{N}$ is the unit normal vector of the freeform curve at the refraction point, and n is the ratio of the refractive index of the lens n_1 to the surrounding air n_0, which is about 1.0. We also plot another light path passing through points A_2 and B_2 to illustrate the process of designing the freeform curve. It's assumed that the distance between B_1 and B_2 is very small and they share the same tangent plane T of the freeform curve. Once the point B_1 is known, T can be further obtained based on Eq. (2) and B_2 can be calculated as the intersection point of tangent plane T and the incident ray $\overrightarrow{A_2B_2}$. Using the same method, other points can be iteratively obtained and the freeform curve can be fitted

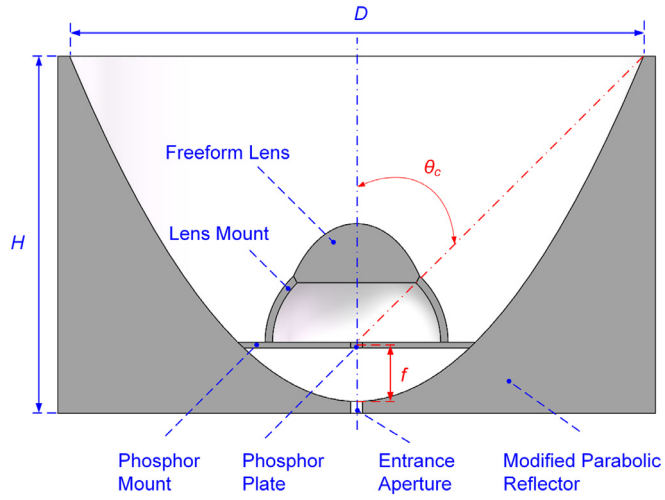

Fig. 7. The 3D structure of the modified parabolic reflector-coupled freeform lens.

by applying the lofting method. The details of designing the freeform curve can be found in our previous study [25].

After obtaining the parabola and freeform curve, we construct the 3D structure of the modified parabolic reflector-coupled freeform lens by rotating the 2D curves along the symmetrical axis. As shown in Fig. 7, the presented optics consists of not only the designed reflector and freeform lens, but also other two mounting parts, namely the phosphor mount and the lens mount. The reflector is designed with an inner paraboloid and a cylindrical shape outside for the convenience of operation. It can be seen that the phosphor mount is supported by the paraboloid and the phosphor plate is mounted in the middle of the phosphor mount. The lens mount, whose inner and outer surface are both spherical surfaces, is positioned on the upper surface of the phosphor mount and is used to support the freeform lens. It should be noted that both the phosphor mount and lens mount need to have high visible light transmittance in order to reduce the light loss due to absorption.

3.3. Simulation results

In this section, the optical performance of the transmissive pc-WLD integrated with the designed optics is evaluated using the simulation method presented above. The paraboloid is set to be a mirror surface with a reflectivity of 0.95. The material of the freeform lens, lens mount, and phosphor mount is PMMA with the refractive index of 1.49 and a high transmission of 0.95 at visible wavelength. The output light along the forward direction is collected by a receiver, which is 1.0 m away from the phosphor plate and has a size of $3.0\,m \times 3.0$ m. In the simulation, the phosphor plate has a diameter of 1.0 mm and a thickness of 0.6 mm.

Fig. 8(a) shows the comparison of the spatial intensity distributions of the blue and yellow lights applying three types of optics. Compared with the divergent distribution of the yellow light presented in Fig. 2, the transformed yellow light distribution exhibits similar Gaussian distribution with blue light, demonstrating the effectiveness of the beam collimation in enhancing the color mixing effect of transmissive pc-WLD. These three types can all achieve the intensity match and the main difference lies in that the absolute value of the yellow light intensity. Compared with type 1, type 2 possesses higher yellow light intensity at small angle because the part of light without being collimated by type 1 is collimated by the freeform lens of type 2, contributing to higher intensity at small angle. Compared with type 2, type 3 has higher intensity at the whole view angles due to the collection of the backward scattering light. The spatial intensity ratio of the yellow light to the blue light, which is also called Y/B ratio, determines the angular correlated color temperature distribution [3]. Fig. 8(b) plots the CCT distribution versus view angle of three optics. It should be noted that only view angles varying from −10° to 10° are plotted because there is no light outside this region, which can be seen in Fig. 8(a). For three types, the CCT distributions are similar, namely the CCT in the middle is higher than that at the edge. Compared with other two types, type 3 has the flattest distribution. The CCT deviations of three types over the view angle are 1570 K, 1133 K, and 734 K, respectively. We define the angular color uniformity (ACU) as the ratio of the minimum CCT to maximum CCT in the whole view angle. The obtained ACU of these three types are 0.71, 0.77, and 0.85, respectively. Therefore, type 3 can effectively achieve small-divergent-angle uniform illumination for the transmissive pc-WLD.

We also evaluate the output optical power and the intensity of the white light on the receiver. As shown in Fig. 9, the reference group denotes the pc-WLD without secondary optics. It can be seen that the blue optical power remains almost unchanged for three cases, whereas the yellow optical power of other three types is obviously higher than that of the reference case. This finding indicates that the secondary optics is mainly re-distributing the intensity distribution of yellow light from large view angle to small view angle. Among these cases, benefitting from reusing the backward scattering light, type 3 has the highest yellow optical power as well as the total optical power. Similarly, type 3 also possesses the highest intensity. Compared with the reference case, the average and maximum intensity are increased by 4.0

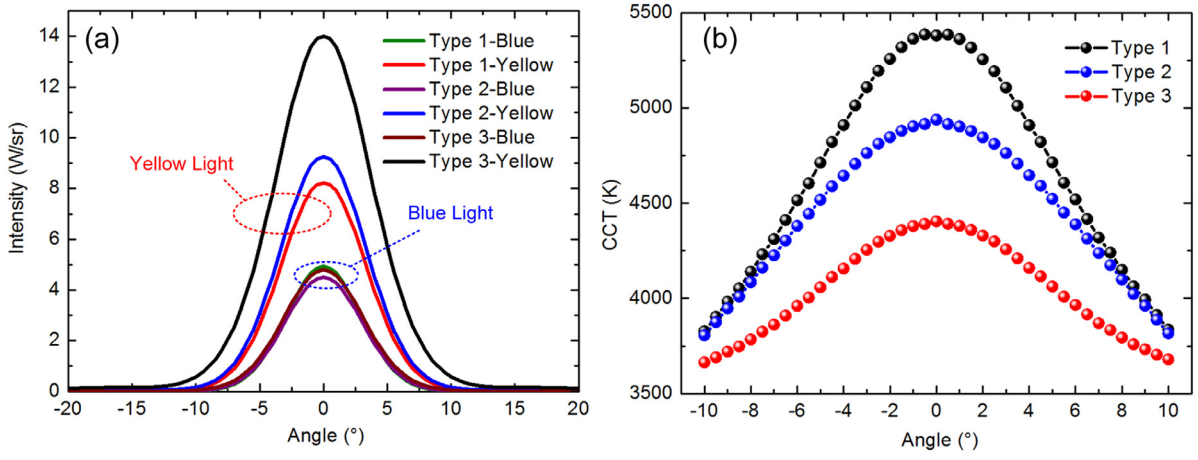

Fig. 8. (a) The spatial intensity of the blue and yellow lights and (b) the spatial CCT distribution of the pc-WLD using three types of optics.

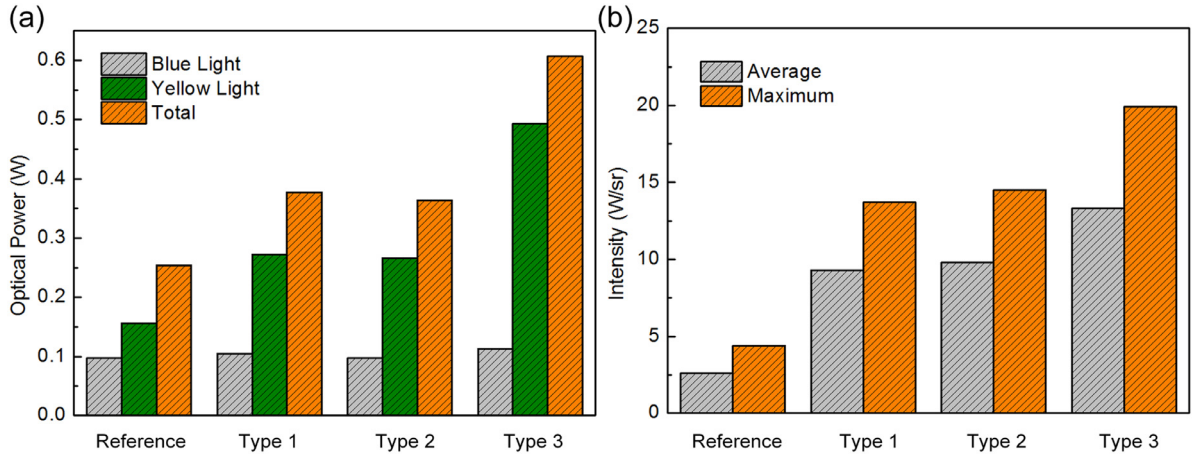

Fig. 9. The comparison of (a) the optical power of the blue light, yellow light, and total light; (b) the average and maximum intensity of the total light for the reference case without optics, and other cases using three types of optics.

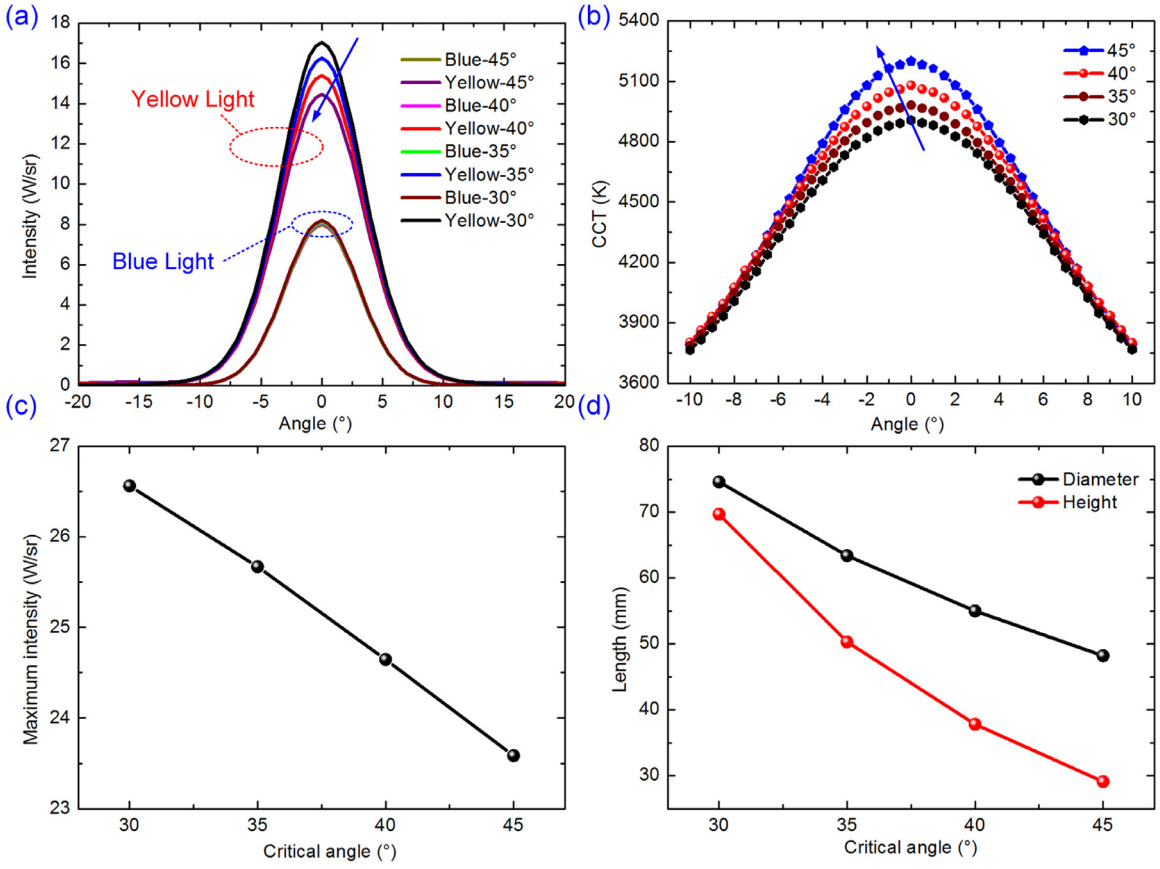

Fig. 10. Effect of the critical angle θ_c on the spatial intensity, spatial CCT, maximum intensity, and whole size of the presented optics.

times and 3.5 times by applying type 3 optics, respectively. Considering the light-emitting area is fixed, the source luminance is proportional to the intensity. Therefore, the presented modified parabolic reflector integrated with the freeform lens can greatly enhance the luminance of the transmissive pc-WLD.

In the following, we discuss the effects of two key size parameters of the presented optics, namely the critical angle θ_c and the focal length f, on the spatial intensity distribution, spatial CCT distribution, maximum intensity, and whole size including the aperture diameter D and the height of the optics H, as shown in Fig. 7. Fig. 10 shows the effect of the critical angle. As θ_c increases from 30° to 45°, the blue light intensity distribution remains almost unchanged and the yellow light intensity keeps decreasing, corresponding to a decreasing Y/B ratio and an increasing CCT in the small-angle region shown in Fig. 10(b). In addition, the rise of θ_c will decrease the maximum intensity. In this case, lower θ_c is more favorable in terms of higher color uniformity and higher luminance. However, as shown in Fig. 10(d), when θ_c is small, the diameter and height of the whole optics is higher, which is against the trend of

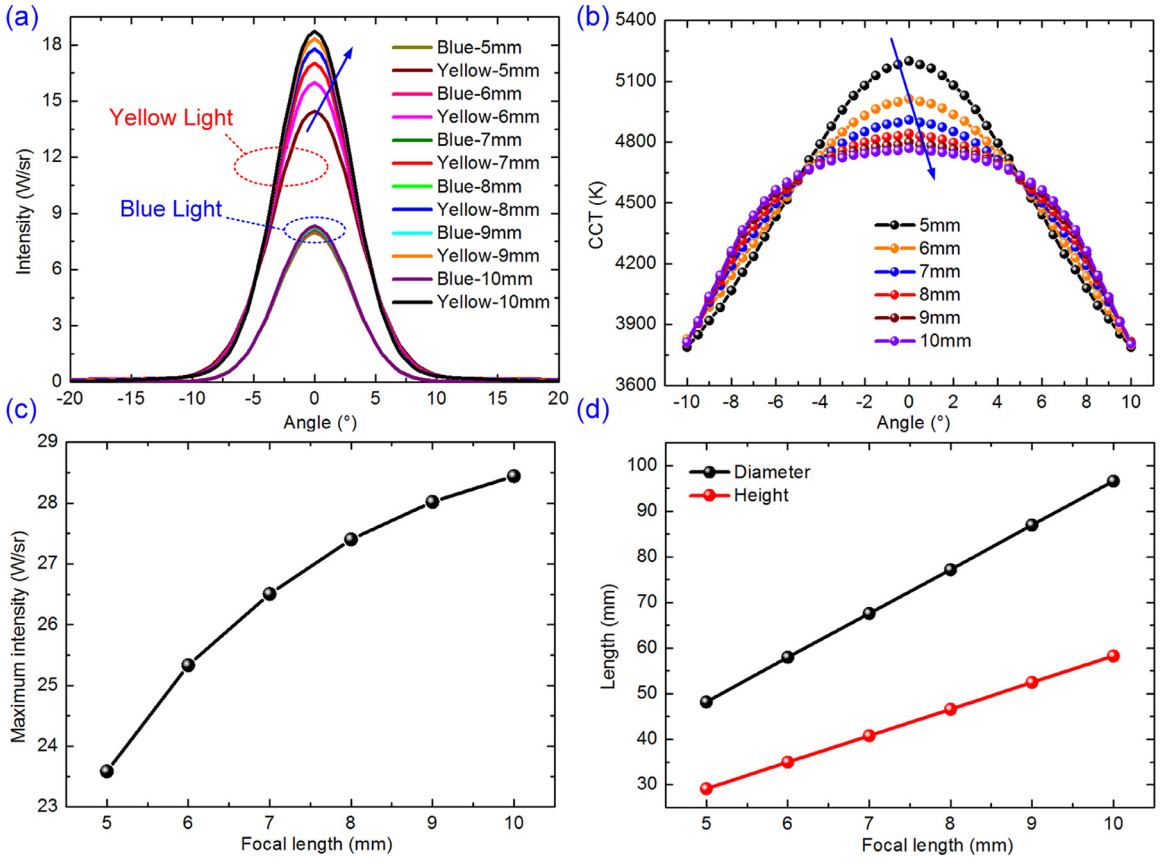

Fig. 11. Effect of the focal length *f* on the spatial intensity, spatial CCT, maximum intensity, and whole size of the presented optics.

developing compact white light sources. Fig. 11 shows the effect of the focal length. As the focal length increases from 5 mm to 10 mm, the yellow light intensity keeps rising, corresponding to a decreasing CCT in the small-angle area shown in Fig. 11(b). The higher focal length will also lend to higher intensity and the whole size of the optics. It can be found that the focal length and the critical angle have opposite effects. As a whole, larger optics has better ACU and higher luminance. This is mainly attributed to two factors. On the one hand, the relative size of the phosphor plate is smaller as the size of the optics increases, in which case the extended source effect is reduced. On the other hand, there is light deflection and total reflection loss when the backward scattering light is reflected back onto the freeform lens and lens mount. The rise of the size of the reflector will reduce the light reflection effect and total reflection loss. In practical application, the tradeoff between them should be evaluated in advance to gain the best benefits.

4. Experimental validation

Finally, we fabricated a porotype of the secondary optics to validate the above findings. The critical angle and focal length are respectively set to be 45° and 5 mm taking precedence to the volume of the optics. As shown in Fig. 12, the reflector is made of aluminum alloy and the inner surface is treated by the vacuum aluminum plating technology to maintain a high reflectivity. The diameter and height of the reflector are 48 mm and 29 mm, respectively. The material of the freeform lens, lens mount, and phosphor mount is PMMA. The phosphor plate with a diameter of 1 mm is positioned in the right middle of the phosphor mount. The assembling of the lens, phosphor plate and reflector is same as the design shown in Fig. 7.

Then, the spatial CCT distribution of the transmissive pc-WLD without and with the fabricated optics are measured using a spectrophotometer (XYC-I, Enci Co. Ltd.) and the results are shown in Fig. 13. For

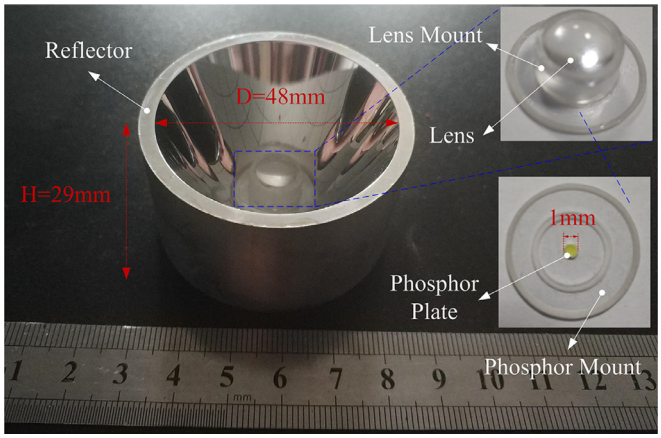

Fig. 12. Photograph of the assembly of the fabricated reflector and freeform lens. The upper inset shows the enlarge figure of the assembly of the lens and phosphor, and the lower inset shows the phosphor plate mounted in the phosphor mount.

the pc-WLD without optics, there is a blue spot on the middle of the illuminated area corresponding to a very high CCT (>10,000 K) in the view angle ranging from −10° to 10°. There is almost yellow light (yellow ring) in the surrounding of the blue spot, corresponding to the low CCT (<4000 K) in the large view angle. This indicates the color mixing effect is very bad and very little white light is generated in this region. After applying the optics, the illumined spot is significantly decreased and the measured view angle is from −10° to 10° due to the light collection. More importantly, there is a white spot corresponding to a very flat CCT distribution. The CCT deviation (998 K) is obviously

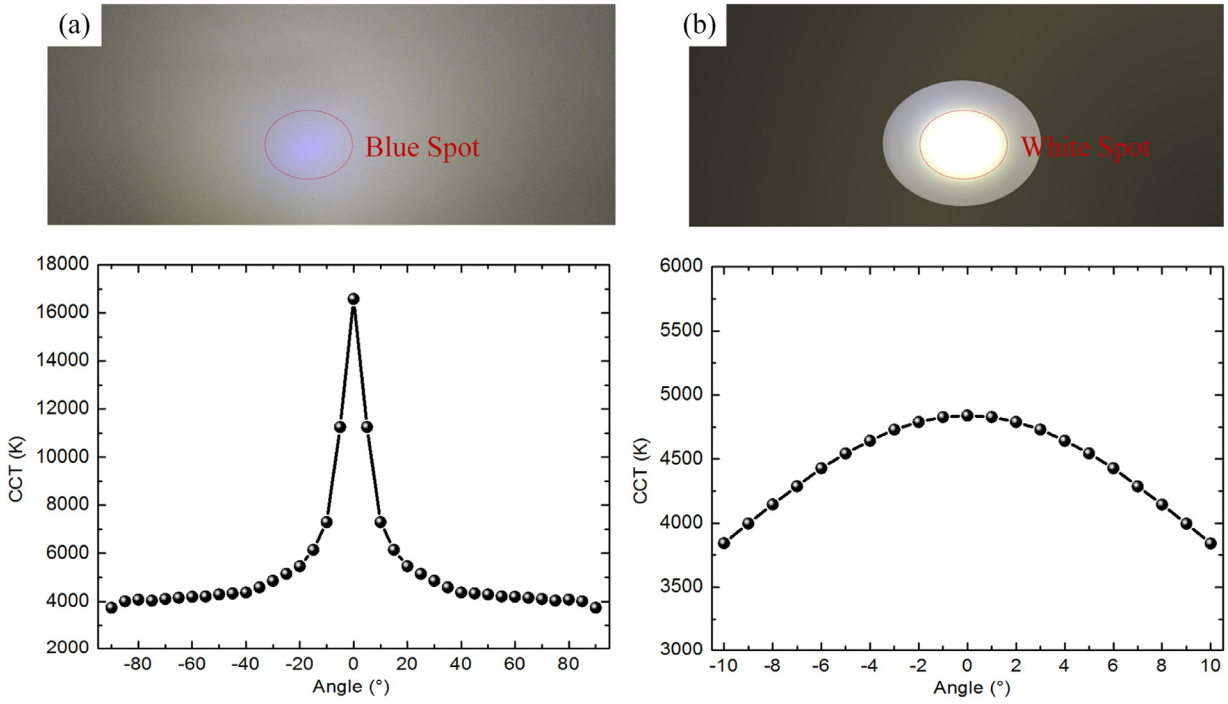

Fig. 13. The photograph of the illuminated spot and the spatial CCT distribution for the transmissive pc-WLD (a) without and (b) with secondary optics.

lower than that of the case without the optics (>10,000 K), demonstrating that the presented optics can achieve a uniform white illumination. The ACU is measured to be 0.80, which is smaller than the simulated value. It is mainly attributed to the assembly error and the mismatch between the parameters used in the simulation and experiment. In addition, the maximum luminance of pc-WLD is measured by a spectral radiance colorimeter (SRC-200M, Everfine), which is positioned to be horizontal to the center of phosphor. It is observed that the measured luminance is increased from 2.36×10^5 cd/m^2 to 1.19×10^6 cd/m^2 after using the fabricated optics. The enhancement is attributed to the reduced divergent angle. Therefore, the experimental results verifies that the presented modified parabolic reflector coupled with freeform lens can simultaneously achieve small-divergent angle uniform illumination and luminance enhancement of the transmissive pc-WLD.

5. Conclusions

In this work, we found the blue spot and yellow ring phenomenon of the transmissive pc-WLD corresponding to a very poor ACU due to the mismatch of the spatial intensity distribution of the blue and yellow lights. To tackle this problem, we presented a parabolic reflector-coupled with a freeform lens to collimate all the rays emitting from the phosphor. The method of constructing the reflector and the freeform lens was illustrated. It's found by the simulation that the divergent intensity distribution of the blue light was transformed into a focused intensity distribution, whereas the focused intensity distribution of the blue light exhibited only a slight change. In this case, we achieved the intensity match and obtained a high ACU of 0.85 with a view angle of ±10°. In addition, the luminance of the pc-WLD was significantly enhanced by nearly four times using the optics due to the collection of the backward scattering light and reduced divergent angle. The effects of the size parameters of the optics were studied and it was found that there was a trade-off between small volume and high ACU. These findings were finally verified by experiments. Therefore, the presented secondary optics may facilitate the development of the high-ACU and high-luminance phosphor-converted laser-based white light source.

Acknowledgments

The authors would like to acknowledge the financial support by National Natural Science Foundation of China (51625601, 51576078, and 51606074), the Ministry of Science and Technology of the People´s Republic of China (Project No. 2017YFE0100600), the financial support from Creative Research Groups Funding of Hubei Province (2018CFA001).

Supplementary materials

Supplementary material associated with this article can be found, in the online version, at doi:10.1016/j.optlaseng.2019.05.022.

References

[1] Luo XB, Hu R, Liu S, Wang K. Heat and fluid flow in high-power LED packaging and applications. Prog Energy Combus Sci 2016;56:1–32.
[2] Ma YP, Hu R, Yu XJ, Shu WC, Luo XB. A modified bidirectional thermal resistance model for junction and phosphor temperature estimation in phosphor-converted light-emitting diodes. Int J Heat Mass Transf 2017;106:1–6.
[3] Ma YP, Wang M, Sun J, Hu R, Luo XB. Phosphor modeling based on fluorescent radiative transfer equation. Opt Express 2018;26(13):16442–55.
[4] Maur MAD, Pecchia A, Penazzi G, Rodrigues W, Carlo AD. Efficiency drop in green InGaN/GaN light emitting diodes: the role of random alloy fluctuations. Phys Rev Lett 2016;116(2):027401.
[5] Wierer JJ, Tsao JY, Sizov DS. Comparison between blue lasers and light-emitting diodes for future solid-state lighting. Laser Photonics Rev 2013;7(6):963–93.
[6] Basu C, Meinhardt-Wollweber M, Roth B. Lighting with laser diodes. Adv Opt Technol 2013;2(4):313–21.
[7] Savastru D, Savastru R, Miclos S, Lancranjan II. Simulation of laser induced absorption phenomena in transparent materials. Opt Laser Eng 2018;110:288–95.
[8] Meng LQ, Huang ZQ, Han ZG, Shen H, Zhu RH. Simulation and experiment studies of aberration effects on the measurement of laser beam quality factor (M2). Opt Laser Eng 2018;100:226–33.
[9] Denault KA, Cantore M, Nakamura S, DenBaars SP, Seshadri R. Efficient and stable laser-driven white lighting. AIP Adv 2013;3(7):072107.
[10] Masui S, Yamamoto T, Nagahama S. A white light source excited by laser diodes. Electron Commun Japan 2015;98(5):23–7.
[11] Cantore M, Pfaff N, Farrell RM, Speck JS, Nakamura S, DenBaars SP. High luminous flux from single crystal phosphor-converted laser-based white lighting system. Opt Express 2015;24(2):A215.
[12] George AF, Al-Waisawy S, Wright JT, Jadwisienczak WM, Rahman F. Laser driven phosphor-converted white light source for solid-state illumination. Appl Opt 2016;55(8):1899–905.

[13] Yang Y, Zhuang S, Kai B. High brightness laser-driven white emitter for Etendue-limited applications. Appl Opt 2017;56(30):8321–5.
[14] Shang BF, Ma YP, Hu R, Yuan C, Hu JY, Luo XB. Passive thermal management system for downhole electronics in harsh thermal environments. Appl Therm Eng 2017;118:593–9.
[15] Zheng P, Li S, Wang L, Zhou TL, You S, Takeda T, Hirosaki N, Xie RJ. Unique Color converter architecture enabling phosphor-in-glass (PiG) films suitable for high--power and high-luminance laser-driven white lighting. ACS Appl Mater Interfaces 2018;10(17):14930–40.
[16] Lee DH, Joo J, Lee S. Modeling of reflection-type laser-driven white lighting considering phosphor particles and surface topography. Opt Express 2015;23(15):18872–87.
[17] Li S, Zhu Q, Tang D, Liu X, Ouyang G, Cao L, Hirosaki N, Nishimura T, Huang Z, Xie RJ. Al_2O_3-YAG:Ce composite phosphor ceramic: a thermally robust and efficient color converter for solid state laser lighting. J Mater Chem C 2016;4(37):8648–8654.
[18] Ma YP, Lan W, Xie B, Hu R, Luo XB. An optical-thermal model for laser-excited remote phosphor with thermal quenching. Int J Heat Mass Transf 2018;116:694–702.
[19] Ma YP, Wang M, Luo XB. A comparative study of reflective and transmissive phosphor-converted laser-based white lighting. In: 17th IEEE intersociety conference on thermal and thermomechanical phenomena in electronic systems (ITherm). IEEE; 2018. p. 773–7.
[20] Wang K, Wu D, Chen F, Liu ZY, Luo XB, Liu S. Angular color uniformity enhancement of white light-emitting diodes integrated with freeform lenses. Opt Lett 2010;35(11):1860–2.
[21] Hu R, Luo XB, Zheng H, Qin Z, Gan ZQ, Wu BL, Liu S. Design of a novel freeform lens for LED uniform illumination and conformal phosphor coating. Opt Express 2012;20(13):13727–37.
[22] Liu ZY, Liu S, Wang K, Luo XB. Measurement and numerical studies of optical properties of YAG:Ce phosphor for white light-emitting diode packaging. Appl Opt 2010;49(2):247–57.
[23] Liu ZY, Liu S, Wang K, Luo XB. Optical analysis of color distribution in white LEDs with various packaging methods. IEEE Photon Technol Lett 2008;20(24):2027–9.
[24] Zhao S, Wang K, Chen F, Wu D, Liu S. Lens design of LED searchlight of high brightness and distant spot. J Opt Soc Am A 2011;28(5):815–20.
[25] Chen F, Liu S, Wang K, Liu ZY, Luo XB. Free-form lenses for high illumination quality light-emitting diode MR16 lamps. Opt Eng 2009;48(12):123002–7.